Probing the Evolution of the Galaxy Interaction/Merger Rate Using Collisional Ring Galaxies

Russell. J. Lavery

Department of Physics & Astronomy, Northern Arizona University, Flagstaff, AZ 86011

Russell.Lavery@nau.edu

Anthony Remijan[1]

Department of Astronomy, University of Illinois, Urbana, IL 61801

aremijan@astro.uiuc.edu

Vassilis Charmandaris[2]

Astronomy Department, Cornell University, Ithaca, NY 14853

vassilis@astro.cornell.edu

Richard D. Hayes[3]

Department of Physics & Astronomy, Northern Arizona University, Flagstaff, AZ 86011

and

Amy A. Ring

Department of Mathematics, Northern Arizona University, Flagstaff, AZ 86011

ABSTRACT

[1]Current address: NASA Goddard Space Flight Center, Earth and Space Data Computing Division, Code 930, Greenbelt, MD 20771

[2]Chercheur Associé, Observatoire de Paris, LERMA, 61 Av. de l'Observatoire, F-75014 Paris, France

[3]Deceased, April 3, 2003

We present the results from our program to determine the evolution of the galaxy interaction/merger rate with redshift using the unique star-forming characteristics of collisional ring galaxies. We have identified 25 distant collisional ring galaxy candidates (CRGCs) in a total of 162 deep *Hubble Space Telescope* Wide Field/Planetary Camera-2 images obtained from the *HST* Archives. Based on measured and estimated redshifts, these 25 CRGCs all lie in the redshift interval of $0.1 \leq z \leq 1$. Using the local collisional ring galaxy volume density and the new "standard" cosmology, we find that in order to account for the number of identified CRGCs in our surveyed fields, the galaxy interaction/merger rate, parameterized as $(1 + z)^m$, must increase steeply with redshift. We determine a minimum value of $m = 5.2 \pm 0.7$, though m could be as high as 7 or 8. We can rule out a non-evolving ($m = 0$) and weakly evolving ($m = $ 1-2) galaxy interaction/merger rate at greater than the 4 sigma level of confidence.

Subject headings: galaxies: evolution — galaxies: formation — galaxies: interactions — galaxies: peculiar — galaxies: statistics — galaxies: high-redshift

1.   Introduction

It is becoming increasingly evident that the interactions between and the merging of galaxies have contributed substantially to the evolution of galaxies, both in terms of their stellar populations and their morphological appearances. Many of the nearby elliptical galaxies we observe in the general field may have been formed as a result of the merging of two large disk systems (Toomre & Toomre 1972; Toomre 1977; Schweizer 1983; Schweizer & Seitzer 1992). The merging of galaxies may also be responsible for the disappearance of the large faint blue galaxy population found in redshifts surveys and galaxy count programs (Carlberg & Charlot 1992; Broadhurst et al. 1992; Colin et al. 1994). And while galaxy interactions and mergers have been associated with large bursts of star formation, there is also evidence that the lack of interactions may also affect the star formation processes in galaxies, as evidenced by the correlation between the lower rates of star formation with fewer companion galaxies found for low surface brightness galaxies (Bothun et al. 1993).

Observationally, there is at least qualitative evidence for an increase in the galaxy interaction rate with redshift based on the increase of several phenomena accepted as resulting from interactions between galaxies. These include the starburst IRAS galaxies (Lonsdale et al. 1990) and quasars (Boyle et al. 1988). Additionally, in the environs of distant rich clusters of galaxies, the presence of an excess of blue star-forming galaxies in these clusters, known as the "Butcher-Oemler" effect (Butcher & Oemler 1978, 1985), is at least partially,

if not totally, the result of interacting galaxy systems (Lavery & Henry 1988; Lavery et al. 1992b; Couch et al. 1994; Dressler et al. 1994).

Several theoretical arguments have also been put forth supporting a steep evolution of the galaxy merger rate as a function of redshift. The parameterization of this evolution is expressed as $(1+z)^m$. Toomre (1977) considered two-body encounters in an $\Omega = 1$ universe and suggested that $m = 2.5$. Carlberg (1990) has suggested that the value of m is sensitive to the value of Ω. Assuming a CDM-like cosmology, Carlberg (1990) has derived the following relationship:

$$m = 4.51 \, \Omega^{0.42}.$$

For $\Omega = 1$, a very steep increase in the interactions and mergers of galaxies with redshift is predicted and this expectation can be tested observationally.

Unfortunately, a direct measure of m has proven to be quite difficult. The main challenge in quantitatively determining the increase of interactions and mergers with redshift is the difficulty of identifying a complete volume sample of such systems, even at moderate redshift. Since tidal features and distortions are, in many cases, weak and of low surface brightness, it is often problematic to observe such features in high redshift galaxies (see Mihos 1995; Hibbard & Vacca 1997).

Due to the problems associated with simply using the disturbed morphological appearance of a galaxy to identify it as having undergone a recent interaction, the observational programs to investigate the evolution of the galaxy interaction rate have been based on determining the evolution of the galaxy pair fraction as a function of magnitude and/or redshift. The evolution of the galaxy pair fraction as a function of redshift has been parameterized as $(1+z)^n$, similar in form to the galaxy merger rate with an exponent n rather than m.

Zepf & Koo (1989) first applied this method to determine this exponent n using deep multi-color plates taken on the KPNO 4-meter Mayall telescope. Based a complete magnitude limited sample of $\sim$1000 galaxies, they found an excess of close pairs of galaxies consistent with a value of n equal to 4.0 ± 2.5. A similar approach using images obtained on the Canada-France-Hawaii Telescope has been undertaken by several investigators. Carlberg et al. (1994, hereafter CPI), determined a value of $n = 2.3 \pm 1.0$ analyzing a sample of $\sim$400 galaxies. Yee & Ellingson (1995) using a sample of $\sim$100 field galaxies with measured redshifts determined a value of $n = 4.0 \pm 1.5$. But, in opposition to these determinations of n is the result of Woods et al. (1995). Their magnitude limited sample of $\sim$900 galaxies was complete at a level of two magnitudes below that of the two previously mentioned CFHT programs, yet Woods et al. (1995) found no evidence for any evolution of the galaxy pair

fraction ($n = 0$). Finally, in the study of 545 field galaxies with an average redshift of $< z > = 0.33$ from the CNOC survey on the Canada-France-Hawaii Telescope, Patton et al. (1997) determined an intermediate value for n, with $n = 1.8 \pm 0.9$.

This significant variation in the value of n cannot be simply attributed to differences in the image resolution of the various data sets. Analysis of a sample of 146 galaxies in a field imaged with the *HST* by Burkey et al. (1994), complete to the same magnitude limit as that of Woods et al. (1995), resulted in a relatively large value for n, with $n = 3.5 \pm 0.5$. Yet, from the Medium Deep Survey *HST* Key project, Neuschaefer et al. (1995), using a sample of $\sim$4500 galaxies, found no excess of galaxy pairs, consistent with a non-evolving ($n = 0$) galaxy pair fraction out to a redshift of 0.5. Interestingly, while CPI and Neuschaefer et al. (1995) have determined very different values for n, 2.3 ± 1.0 and $\sim$0 respectively, they have both determined the observed faint galaxy pair fraction to be $\sim$14%! The difference in their values for n results from the determination of the correction for non-physical galaxy pairs. with CPI estimating $\sim$4% to be non-physical pairs and Neuschaefer et al. (1995) estimate the correction to be 13%.

Besides the difficulty in determining the value of n for the evolution of the galaxy pair fraction, relating n to the exponent used for the evolution of the galaxy merger rate, m, is not straightforward, as it is *extremely difficult to estimate what fraction of the galaxy pairs which may show a disturbed morphology will actually lead to a violent interaction of a merger.* Burkey et al. (1994) suggest the z derivative of the pair fraction should represent the galaxy merger rate, meaning $m = n - 1$. But, if the ratio of merger timescales at different epochs is taken into account, as was done by CPI, the merger rate exponent, m, is approximately equal to $n + 1$. Zepf & Koo (1989) and Yee & Ellingson (1995) argue that the evolution of the galaxy merger rate should be quite similar to that of the galaxy pair fraction, implying $m = n$.

Because of these difficulties with the analysis of distant galaxy pairs, several research groups have utilized the high-resolution imaging capabilities of the *HST* to quantify the galaxy merger rate at high redshift. Based on a sample of 285 galaxies with redshifts out to $z = 1$, Le Fèvre et al. (2000) used visual classifications of galaxies along with a galaxy pair analysis to determine a value for m of 3.4 ± 0.6 (for comparison with more recent results, it should be noted that this value was determined assuming $q_0 = 0.5$ and would be lower in the new "standard" cosmology). For even higher redshifts, Conselice et al. (2003) have used a statistical measure of the asymmetry of a galaxy to quantify the number of galaxy mergers as a function of redshift. Using galaxies in the *Hubble Deep Field*, they find a steep evolution of the galaxy merger rate for massive, luminous galaxies out to $z \sim 3$, with a value for m in the range of 4 to 6. The importance of the image resolution provided by the *HST* cannot be

understated and we have also utilized this capability to investigate distant collisional ring galaxies.

Collisional ring galaxies (CRGs) are a relatively small fraction of all galaxies that have undergone a recent interaction, being produced in the relatively rare circumstance of a small galaxy passing directly through the center of a disk galaxy. The "Cartwheel" galaxy (Zwicky 1941) is probably the most well-known example of this type of galaxy. A thorough review of the properties of collisionally produced galaxies is given by Appleton & Struck-Marcell (1996). While the ring structure of these galaxies identifies them as galaxies having undergone a recent interaction, at redshifts of $z \sim 0.5$, these galaxies will be only several arcseconds in diameter and difficult to identify with even the best image resolution obtainable with ground-based observatories.

Collisional ring galaxies have several advantages for investigating the evolution of the galaxy interaction rate:

1. The signature morphological appearance of CRGs, a high surface brightness knotty ring, makes it possible to identify them at high redshift ($z \leq 1$) given the high image resolution obtainable with the *HST*.

2. The ring structure, delineated by regions of massive star formation, is a *direct* result of the dynamical process of interest. The uncertainty in how m and n are related is avoided.

3. The timescale for the presence of the ring structure is short (1 or 2 dynamical times), meaning the interaction was a recent event.

4. The ring structure will only be produced by an "intruder" galaxy that has a significant mass compared to the "target" galaxy (at least 10%). Therefore, only events that will have a significant effect on the morphological appearance of the galaxy are investigated.

In this paper, we present the results from our program to identify distant collisional ring galaxy candidates (CRGCs) in deep WFPC2 images obtained from the *HST* Archives. Our search method and results, the identification of 25 distant CRGCs, and the spectroscopic observations of several of these CRGCs are presented in Section 2. In Section 3, we discuss the implication of these results on the redshift evolution of the galaxy interaction/merger rate, with Section 4 being a discussion of corrections and possible biases affecting our value for m. Our conclusions, consistent with the "work-in-progress" results presented in Lavery & Remijan (2000), are summarized in Section 5.

2. Observations

2.1. *Hubble Space Telescope* Data

The concept for this program originated from the results of Lavery et al. (1996) who found a high density of distant CRGCs lying behind the Local Group dwarf spheroidal galaxy in Tucana (Lavery & Mighell 1992). The data of Lavery et al. (1996) consisted of two deep images, with total exposure times of 3.5 and 4 hours, in the broad *HST* F814W filter. With these long exposure times in mind, our initial selection of WFPC2 fields to be searched for CRGCs were pointed observations (PIs: Couch, Dressler, Ellingson, Miley and Stockton) of distant clusters of galaxies and distant radio galaxies which were obtained from the *HST* Archives. The only constraint, besides exposure time, on the field selection was that at least one set of observations were made through one of the broad *HST R*-band or *I*-band filters (F606W, F622W, F702W, F814W). This filter constraint was chosen so that the identification of the CRGCs would be based on their appearance in the rest-frame *B*-band. The *Hubble Deep Field* was also included in this sample. These pointed observations provided a total of 43 WFPC2 fields.

Based on the experience gained from the analysis of the pointed observations, we found that fields with exposures times greater than 4000 seconds would have a sufficient signal-to-noise ratio for the classification of distant galaxies as CRGCs. With this constraint, a total of 118 WFPC2 fields were obtained from Parallel Observation Programs (PI: Griffiths, Windhorst). These fields, along with the pointed observations, provided a sample of 162 WFPC2 fields in total.

The identification of the CRGCs was done through visual inspection of the processed frames (after cosmic ray removal and image addition). Each field was searched independently by some combination of three of the authors (RJL and two others). After completion of the independent identifications, the candidate lists were compared and a consensus was reached on those objects to be included in our final CRGC list.

Visual inspection was done rather than employing an automated identification routine for several reasons. First, the number of objects being searched for is very small compared to the total number of objects that would need to be structurally analyzed. Roughly expecting about 1 CRGC in every 10 WFPC2 fields, several hundreds of galaxies would have to be analyzed. While distinguishing between exponential disks and de Vaucouleurs profiles can be done, the construction of algorithms for the identification of coherent ring structure is much more complex. Second, it would still be necessary for visual classification to distinguish the P-type and O-type rings and to determine the presence of any weak bar-like or spiral structure. Additionally, the reimaging optics in WFPC2 camera system produce ring shaped

artifacts due to bright stars in the field of observation. These ring artifacts have a knotty structure and look like face-on empty collisional ring galaxies. Their location with respect to the bright star varies in both the distance from the star and its angular position, depending on the location of the star on the CCD chip. But, fortunately, these "ringers" can be identified as artifacts as a line drawn from the center of the CCD through the bright star will bisect the ring-shaped image produced by that star.

To provide consistency between the classifiers in the visual identification process, the "reclassification" of the collisional ring galaxies in the Few & Madore (1986, hereafter FM86) sample of ring galaxies was independently done by the classifiers prior to inspecting the WFPC2 fields. The FM86 sample of ring galaxies contains 69 objects consisting of two types: O-type or resonant rings and P-type or collisional rings. Resonant or O-type rings, which comprise ∼40% of the FM86 sample, have a smooth structure and a centrally located nucleus. The P-type or collisional rings, which exhibit a ring with a crisp knotty structure and sometimes have a displaced nucleus, constitute the remaining ∼60% of the FM86 sample. A total of 50 galaxies were selected, consisting of the 41 P-type ring galaxies in the FM86 sample along with 9 of their O-type ring galaxies, and were "reclassified" independently and without prior knowledge of the FM86 classifications, by each visual inspector using extracted images from the Digitized POSS. For the 9 O-type rings in this sample, there was strong agreement with the FM86 classification. But, of the 41 P-type rings, unanimous agreement with the P-type ring classification was reached for only 14 galaxies, with 2/3 of the galaxies not being classified as P-type by the authors of this paper. Most of the discrepancy was due to either the presence of spiral structure, which produced a ring-like appearance, or the presence of a galactic bar which has induced a ring-like structure more consistent with the O-type ring morphology.

We reached two important conclusions from this reclassification exercise. First, our classification of galaxies as P-type rings is very conservative. This gives us confidence in our ability to identify CRGCs that have a high likelihood of being true CRGs implying that our sample will not be contaminated by misclassified "normal" galaxies. Second, based on our reclassification of the FM86 sample, in which we found only 14 of the 41 to meet our criteria for being P-type ring galaxies, the local CRG volume density may only be 1/3 of that determined by FM86.

The result of our visual inspection of 162 WFPC2 fields is a total of 25 distant CRGCs, for which images of 20 are presented in Figure 1. The photometric properties of our 25 CRGCs is presented in Table 1. For the photometric calibration, we have adopted the standard photometric zero-points and color coefficients determined by Holtzman et al. (1995). As a number of our CRGCs were identified in Parallel fields, they were only observed in a

single filter. Eight of our CRGCs were observed in two filters allowing for color measurements for which we find an average (V-I) color of 1.59 ± 0.15. As we will be using V-band magnitudes of the CRGCs to estimate their redshifts, for those CRGCs with only a single observation, we have adopted colors of (V-I) = 1.5 and (V-R) = 1.0 in order to determine standard V-band magnitudes. These magnitudes should be accurate to ±0.1 mag.

2.2. Optical Spectroscopy

Optical spectroscopy for several of our CRGCs was obtained on 21 January 2002 using the Double Spectrograph at the Palomar[1] 5-m Hale telescope. Complete spectral coverage from 4000 to 8000 Å was obtained by using dichroic filter #55 with a transition wavelength at 5500 Å, to split the light into a blue and red beam. In the blue beam, the 600 l/mm grating was used to observe the wavelength range of 4000 to 5800 Å with a dispersion of 1.73 Å/pixel and a resolution of ∼4 Å. In the red beam, which covered the wavelength range of our main interest, we used the 316 l/mm grating resulting in a dispersion of 2.44 Å/pixel over the wavelength range of 5500 to 8000 Å. A slit width of 1 arcsec was used which produced spectral resolution of ∼5 Å. Both sides of the spectrograph were equipped with a thinned 1024×1024 Tek CCD. Each CCD had a gain of 2.0e- per DN with a readout noise of 8.6e- for the blue beam and 7.5e- for the red beam.

The spectra were reduced and analyzed with the IRAF[2] package. The spectral reduction included bias subtraction, scattered-light corrections, and flat-fielding with dome flats. The two-dimensional images were rectified based on the arc-lamp observations and the trace of standard stars. Relative flux calibration was obtained by observations of standard stars from the list of Oke (1990). Since the night was non-photometric, only the standard stars observed contiguous to our targets were used to generate the sensitivity function. The results of the spectroscopic observations of our four CRGC targets follow.

---

[1]Observations at the Palomar Observatory were made as part of a continuing cooperative agreement between Cornell University and the California Institute of Technology.

[2]IRAF is distributed by the National Optical Astronomy Observatories, which are operated by the Association of Universities for Research in Astronomy, Inc., under cooperative agreement with the National Science Foundation.

2.2.1. CRGC 5

CRGC 5 lies in close proximity to the x-ray cluster MS0440 + 0210 ($z = 0.190$) and was identified as a possible gravitational arc (A1) by Luppino et al. (1993). Spectroscopic observations of A1 by Gioia et al. (1998) produced a redshift of 0.5317, suggesting it may be weakly lensed by the foreground cluster. We observed CRGC 5 for a total exposure time of 3600 seconds. Several strong emission lines indicative of significant star formation in progress, specifically [O II] λ3727, Hβ, and [O III] λ5007, are present (see Figure 2). These three lines give a redshift of 0.5322 ± 0.0005, consistent with the redshift obtained by Gioia et al. (1998).

2.2.2. CRGC 10

CRGC 10 was observed for a total of 9000 seconds. A single strong emission line at 7679.0 Å is present (see Figure 2). We tentatively identify this line as Hβ leading to a redshift of 0.580. If this Hβ identification is correct, then other strong emission lines, unfortunately, fall directly on night sky emission lines. The line of [O II] λ3727 falls atop the strong line of sodium D at 5890 Å and the line of [O III] λ5007 falls on the night sky line at 7913.7 Å. This night sky line at 7913.7 Å is just a medium strength emission line. The resultant sky subtracted spectrum does show an excess at this wavelength possibly due to the presence of [O III] λ5007 in the spectrum of this galaxy. The alternative identification of the emission line at 7679.0 Å as [O II] λ3727 would result in a galaxy redshift of 1.06. Our estimated redshift for CRGC 10 (see Section 3.1) is 0.85, lying between 0.580 and 1.06. But, given the relative brightness of the apparent "intruder" galaxy, it seems more likely that CRGC 10 is an under-luminous galaxy at $z = 0.580$ rather than an over-luminous galaxy at $z = 1.06$.

2.2.3. CRGC 7 and CRGC 11

These two CRGCs were observed for 7200 seconds and 4800 seconds, respectively. For CRGC 7, a weak continuum is present. An extremely weak emission line-like feature is present in the 2-dimensional images, but its presence in the extracted 1-dimensional spectrum is not easily revealed. At the pixel location measured in the spectral image, there is a feature with a peak similar to the larger noise peaks but with a width unlike the noise peaks in being several pixels in width. This feature is of interest as it shows a tilt which may be indicative of rotation andor expansion velocity of the galaxy. Identifying this weak feature as [O II] λ3727 leads to a redshift of 0.629, which is uncertain, but very close to the estimated redshift

of 0.68 for this CRGC. Lastly, the extracted spectrum of CRGC 11 reveals no information about this galaxy.

3. Discussion

3.1. Estimated Redshifts for the CRG Candidate Sample

Our goal in identifying this sample of distant CRGCs is to determine the value of m, the exponent used to quantify the evolution of the galaxy merger/interaction rate with redshift. In order to accomplish this, either individual redshifts for our CFGC sample or the redshift interval in which these CRGCs lay is required. At this time, measured redshifts are available for only five of the 25 CRGCs in our sample. However, we have been able to constrain the redshift interval of our sample based on estimated redshifts for the remaining 20 CRGCs.

We have used the sample of 11 collisional ring galaxies studied by Appleton & Marston (1997) to determine an "average" absolute V magnitude, using a value for the Hubble Constant of $H_0 = 71$ km s^{-1} Mpc^{-1}. Extinction corrections and k-corrections to the apparent V magnitudes were made by Appleton & Marston. The resulting absolute V magnitudes for these galaxies were averaged to determine a "standard" absolute V magnitude of M_V = -21.1 $\pm$ 1.1 for this sample. While this sample of CRGs is not a statistically complete sample, it was selected to be a representative sample. This value of M_V is consistent with an L* galaxy having several tenths of a magnitude increase in luminosity due to the star formation associated with the ring structure. This may also indicate that similar to spiral structure, the target galaxy must be relatively large for the development of a coherent ring structure.

We have calculated the expected apparent V magnitude as a function of redshift for an M_V = -21.1 galaxy. The k-correction values used were that of an average Sc galaxy (Pence 1976) and we have assumed an average V-band galactic extinction, A_V, of 0.1. The cosmological parameters (H_0, Ω_M, Ω_k, and Ω_Λ) and the values used are discussed in more detail in Section 3.2. The estimated apparent V magnitude as a function of redshift is shown in Figure 3. Based on this m_V-z relation, estimated redshifts for our sample of 25 CRG candidates were determined and are given in Table 1.

As part of several unrelated observational programs, measured redshifts have been published for four of the CRGCs in our sample: CRGC 2 at $z = 0.454$ (3C295 #122, Dressler & Gunn 1983), CRGC 3 at $z = 0.561$ (HDF 3-773.1, Cohen et al. 1996), CRGC 5 at $z = 0.532$ (MS 0440+0204 A1, Gioia et al. 1998), and CRGC 20 at $z = 0.996$ (3C 280, Spinrad at al. 1985). Our spectroscopic observations have confirmed the redshift for CRGC 5 and added

a redshift for a fifth CGRC, CGRC 10 at $z = 0.580$. For this group of five CRGCs, the agreement between our estimated redshifts and the measured redshifts is reasonably good (see Table 1) and provides support for our assumption that this sample of CRGCs lie in the redshift interval of $0.1 \leq z \leq 1$.

3.2. The Evaluation of m

Given that we have been able to constrain the redshift interval in which our CRGCs lie, it is possible to compare the number of CRGCs we have identified with that expected for various values of m, the galaxy merger rate exponent. Using the formalism presented in Carroll, Press, & Turner (1992), the co-moving volume element as a function of redshift is given by

$$dV \;\; = \;\; \frac{c}{H_0(1+z)^2} \; \frac{D_L^2}{(\Omega_M(1+z)^3 + \Omega_k(1+z)^2 + \Omega_\Lambda)^{1/2}} \; d\Omega \; dz \tag{1}$$

where D_L is the luminosity distance for a redshift z. In a flat universe, D_L can be evaluated using the integral expression

$$D_L = \frac{c(1+z)}{H_0} \int_0^z [(1+z)^2(1+\Omega_M z) - z(2+z)\Omega_\Lambda]^{-1/2} \; dz. \tag{2}$$

(see Carroll, Press, & Turner (1992) for the more general expression).

The parameters in these formulae are c, the speed of light, H_0, the Hubble constant, $d\Omega$, the solid angle element, and dz, the redshift interval. The three subscripted omega terms are used to parameterize the expansion properties of the Universe where Ω_M, Ω_k, and Ω_Λ are the fractional contributions due to matter, curvature, and the cosmological constant (dark energy), respectively. These three omega terms are related as such,

$$\Omega_M + \Omega_k + \Omega_\Lambda = 1 \tag{3}$$

with $\Omega_0 = 1 - \Omega_k$. Presently, the best determined values for these cosmological parameters imply a flat ($\Omega_0 = 1$, $\Omega_k = 0$) universe with $\Omega_M = 0.27$, $\Omega_\Lambda = 0.73$, and $H_0 = 71$ km s^{-1} Mpc^{-1} (Bennett et al. 2003).

The total solid angle of sky, $d\Omega$, that we have scanned is equal to the angular area of 162 WFPC2, each consisting of three 800×800 CCDs. The linear image scale for the Wide

Field CCDs in the WFPC2 camera is 0.10 arcseconds per pixel. We did not include the higher resolution PC field in our scanned area due to the lower signal-to-noise ratio of the data in this CCD. Each WF CCD images a solid angle of 1.50×10^{-7} str. With a total of 486 individual CCD images, the total solid angle, $d\Omega$, is equal to 7.31×10^{-5} str. We have not applied any correction to this solid angle, which would be a reduction of approximately 10%, for the area obscured by bright stellar images or the area on each CCD (approximately 30 rows and 30 columns) affected by the WFPC2 reimaging mirrors.

For the local collisional ring galaxy volume density, we have used the value determined by FM86 of $5.4 \times 10^{-6} \ h^3 \ \mathrm{Mpc}^{-3}$ (see Section 4.1), where $h = H_0/100$ km s^{-1} Mpc^{-1}. In their determination of the local volume density, FM86 applied a correction of 20% to their observed value to account for edge-on systems which would not be identified as ring systems due to their inclination. Therefore, for our estimates of the expected number of CRGs, we have reduced the FM86 value by 20%. This gives a value of $4.3 \times 10^{-6} \ h^3 \ \mathrm{Mpc}^{-3}$. We stress here that we have *not* introduced any correction due to our reclassification of the P-type rings (see Section 2.1).

Using equations 1 and 2, we have integrated the product of the co-moving volume element, the local collisional ring galaxy volume density, and the galaxy merger rate parameter of $(1+z)^m$ over the redshift interval of $0.1 \leq z \leq 1$. This produced the expected number of CRGCs in our survey solid angle for various values of m, the results of which are presented in Table 2.

It is interesting to note that since the local collisional ring galaxy volume density is a function of H_0^3 and the co-moving volume element is a function of H_0^{-3} *our estimate of the number of CRGCs is independent of the value of H_0.* For an $\Omega_M = 0.27$, $\Omega_\Lambda = 0.73$ universe, our identification of 25 CRGCs is consistent with an exponent value of $m = 5.2$, suggesting a very steep increase in the galaxy merger/interaction rate with redshift. Given our relatively large sample, we can assume our Poisson distribution can be represented by a Gaussian distribution with 1σ error bars being equal to $N^{0.5}$. In this case with $N = 25$, we find $m = 5.2 \pm 0.7$. We rule out a non-evolving ($m = 0$) and a slowly evolving ($m = 1$-2) galaxy interaction/merger rate at greater than the 4σ level of confidence.

We wish to emphasize two important points. First, our steeply increasing galaxy merger rate is not very sensitive to the possible misclassification of several non-collisional ring galaxies as collisional rings. Even if the contamination were as high as 50%, the value of m would decrease from 5.2 to 4.0, still a very steeply increasing galaxy merger rate. Second, in our determinations for the expected number of CRGs for various values of m, we have used the FM86 value for the CRG volume density. Our "reclassification" of the P-type rings in their sample would reduce the local CRG volume density by a factor of three, decreasing the

expected number of CRGCs in our *HST* fields by the same factor.

This value for m of 5.2 ± 0.7 is consistent with that of Conselice et al. (2003) ($m \sim$ 4-6 for luminous galaxies in the *HDF*), but it is significantly higher than that of Le Fèvre et al. (2000) and the most recent analysis based on galaxy pairs by Patton et al. (2002) of m = 2.3 ± 0.7. It is possible that in addition to the galaxy merger rate, our large value of m may also be indicative of the evolution of several other galaxy properties. First, evolution of the types of orbits for the intruder galaxy may be important. If the distribution of orbits of the intruder galaxies has evolved, with low angular momentum being more common in the past, this would increase the likelihood of interactions that produce ring galaxies (C. Struck, private communication). Second, evolution of the morphological distribution of the general field population of galaxies, specifically a higher fraction of gas-rich disk systems compared to the field today. Unless the system being affected by the intruder galaxy is relatively gas-rich, the interaction will not produce the star formation that delineates the ring structure. If many of the nearby elliptical galaxies are the result of the merger of two disk systems, the exhaustion of gas in the process of forming these galaxies will mean that any subsequent interaction will not lead to enhanced star formation or a ring structure.

4. Corrections and Potential Biases

In order to quantify the evolutionary rate of any astronomical process, it is necessary to compare local samples with distant samples. This is not always straightforward, as the properties of local samples are not always well-determined, and non-representative results can occur if any introduced biases are not taken into account. In this sections, we evaluate various corrections and possible biases and their affect on our result.

4.1. The Local Volume Density

In order to use our sample of distant CRGCs to estimate the exponent m which is used to parameterize the galaxy interaction/merger rate, it is necessary to know the local volume density of collisional ring galaxies. In our determination of the value of m, we have used the collisional ring galaxy volume density of FM86. This local density is based on ring galaxies identified in the *Catalogue of Southern Peculiar Galaxies and Associations* (Arp & Madore 1987), an approximately complete sample of 214 objects out to a survey depth for rings of 10 arc-seconds or larger of $278 \times h^{-1}$ Mpc. This sample is therefore not magnitude limited, but angular size limited with roughly 10 resolution elements across the smallest galaxies. The

214 rings from the *CPGA* consisted of both O- and P-type rings. FM86 classified a random subset of 69 galaxies, selected upon their availability on A-grade SERC (J) blue-light plates, into O- and P-type (40% and 60%, respectively) rings. Applying this division to the total sample of 214 galaxies, they derived a local ring galaxy volume density of of 5.4×10^{-6} h^3 Mpc^{-3}. This value is consistent with the previous, though less rigorous, determination of Freeman & de Vaucouleurs (1974) of 7×10^{-6} h^3 Mpc^{-3}, but is lower than that determined by Thompson (1977), 20×10^{-6} h^3 Mpc^{-3}. This larger value is suspect as the survey fields of Thompson (1977) were located near or on Abell clusters and a number of the identified objects are quite small and may not actually be ring galaxies (Appleton & Marston 1997).

To be able to compare our distant sample of CRGCs with the local sample, it is necessary to ensure consistency in the identification process for both samples. This was done in two ways. First, to ensure that our distant CRGC sample was identified in approximately the same rest-frame wavelength range as FM86, who used the SERC J plates for their ring galaxy classifications, our search and identification process was done only on those WFPC2 images obtained in the broad red wavelength filters (F602W, F622W, F704W, and F814W), which would be similar to the B-band in the rest-frame of our sample. Second, as mentioned earlier, as part of insuring consistency between classifiers, each classifier looked at a sample of 50 ring galaxies from the FM86 sample and typed them as either O-type (resonant) rings or P-type (collisional) rings. While each classifier typed the 9 O-rings in the sample as such, many of the P-rings typed by FM86 were not. With a very narrow range of ±1 galaxy, each classifier typed only 14 of the 41 galaxies as P-rings.

In our determination of m, we have used the local volume density of FM86, presently the best determined value. However, based on our re-classifications of the CRGs in the local sample, we have used much stricter criteria in identifying the distant sample of CRGCs. There is a factor of ~3 difference in the number of rings classified as P-type by FM86 and by us. If this factor of 3 is applied, thereby lowering the local collisional ring galaxy volume density by this factor, the result is a larger value of m, with $m = 7.0$.

4.2. The Survey Area

In our determination of the solid angle covered in our survey, we have used an image scale of 0.1 arcseconds per pixel with the dimensions of each of the three low-resolution CCDs being 800 × 800 pixels. But, due to the reimaging optics of the WFPC2, regions along two sides of each CCD are not illuminated by the sky. The regions are L-shaped strips along the edges of each CCD with a width of ~30 pixels. Therefore, the imaging area of each CCD is actually only 770 × 770 pixels, reducing the survey solid angle by ~7.5%. In addition,

some area was lost due to bright stars and nearby galaxies, which we estimate to be a few percent. Overall, these factors combined lead to a reduction of the survey solid angle by $\sim 10\%$. Correcting for this lost area leads to an increased value of m of ~ 0.15.

4.3. Incompleteness

Incompleteness can enter into and affect our distant CRGC sample in two ways: bright CRGCs overlooked in our visual search and distant CRGCs missed due to being of low signal-to-noise. Any aspect of incompleteness will result in our underestimating the number of distant CRGCs, leading to an increased value for m. But, from Table 2, it can be seen that the expected number of CRGs increases dramatically for large values of m, close to a factor of two for each integer change in the value of m. Therefore, to greatly affect the value of m, the level of incompleteness must be significant.

Our visual search for CRGCs was done independently by several different groups of three of the authors in all of the fields. In the identification of our distant CRGC sample, there was only 1 CRGC out of the 25 that was identified by a single person. This was CRGC 12, which was overlooked due to its relatively high surface brightness. This occurred early in our search and led to greater care in examining the full dynamic range of the images. The remaining 24 CRGCs were identified by at least two searchers, with the large majority being identified by all three searchers. For this reason, we feel confident in the thoroughness of our visual search process.

The second aspect that contributes to possible incompleteness are the distant CRGCs not identified due to their low signal-to-noise in the available images. To evaluate this incompleteness level, we have divided our sample of CRGCs into 4 redshift bins to compare it with the expected redshift distribution based on the combination of volume and evolutionary rate. Figure 4 shows the percentage distribution with estimated redshift determined for our sample (cross-hatched histogram) along with the expected distribution (dotted-line histogram) based on the evolutionary model. There would appear to be a significant deficit of objects in the most distant redshift bin.

While it may be possible to estimate the number of CRGCs missing from the highest redshift bin, the simplest approach to account for this incompleteness is to reduce the redshift interval over which we integrate to determine the value of m. If we disregard the last redshift bin due to incompleteness, this leads to a reduction of the number of CRGCs from 25 to 21 (the 16% in the last redshift bin represents 4 CRGCs) out to a maximum redshift of 0.8 rather than unity. This leads to a value of $m = 6.8$, a significant increase.

However, we must qualify this simple approach. We initially determined the estimated redshifts for our sample of CRGCs simply to place a constraint on the redshift range over which the integration for determining the value of m was conducted, namely that the redshifts of our sample were less than 1. But, the errors associated with these estimated redshifts are relatively large for several reasons. First, we have assumed for our distant sample an absolute magnitude of $M_v = $ -21.1, which was determined using a sample of nearby collisional ring galaxies. This local sample had a scatter of ± 1 magnitude about this average value, which introduces an error of 0.1 to 0.15 in the estimated redshifts. Additionally, the estimated redshifts are quite sensitive to the assumed k-correction. While we have used the k-corrections for an Sc galaxy, the use of the k-corrections for an Scd galaxy leads to estimated redshifts larger by approximately 0.07 and increases the fraction of galaxies in the most distant redshift bin from 16% to 36%! This still indicates some level of incompleteness in the most distant redshift bin, though not as severe. Once again, excluding the most distant redshift bin leads to a sample size of 16 CRGCs with $z \leq 0.8$ and a value of $m = 6.2$.

4.4. Parallel/Pointed Observations

Our sample of 162 WFPC2 fields consists of two very different types of observations: parallel fields and pointed observations. The parallel WFPC2 fields were exposed while other HST instruments were in primary use and should, therefore, constitute a random sampling of distant field galaxies. There are 118 parallel fields in our total sample. The remaining 44 fields are pointed observations towards distant radio galaxies and clusters of galaxies. These pointed fields were part of the initial field sample due to their long exposure times and depth. Clusters of galaxies are regions of high galaxy density and radio galaxies may have an excess of field galaxies associated with them. Is it possible the inclusion of these fields has produced our high value for m?

Overall, there is no excess of CRGCs in the pointed fields compared to the parallel fields. The 118 parallel fields account for 73% of our surveyed solid angle. Based on this percentage, there should be 18.2 CRGCs in the parallel fields and we have identified 17 CRGCs, a difference that is not statistically significant.

Our WFPC2 sample contains 26 pointed observations towards radio galaxies. Observations of the environments of distant radio galaxies suggest $\sim$25% of such radio galaxies are in "rich" (Abell richness 0, 1) clusters of galaxies (Harvanek et al. 2001; Yates et al. 1989; Hill & Lilly 1991; Zirbel 1997). Inspection of our radio galaxy fields does not reveal a relatively large enhancement of field galaxies clustered with the targeted radio galaxies. Much more likely is an enhancement in the field galaxies associated with the radio galaxies by factors

of only 2 to 5, which would not be obvious by inspection. But, such an excess would have only a small affect on our results. To be associated with the radio galaxy, the field galaxies would have to have an almost identical redshift to that of the radio galaxy, as this relatively small galaxy density enhancement must have a low velocity dispersion (200-300 km s^{-1}). We have calculated the volume associated with a redshift interval of ± 0.05 for the redshifts of 0.35 to 0.95 with increments of 0.1 in redshift. This interval of ± 0.05 is equal to a velocity relative to the radio galaxy of $1500/(1 + z)$ km s^{-1}, which is approximately 3 to 4 times the expected velocity dispersion. The percentage of the volume associated with $z \pm 0.05$ to our total volume ranges from 0.6% at $z = 0.35$ to 2% at $z = 0.95$. Given this small fraction of volume with respect to the total volume along the line-of-sight, enhancements of the field galaxy density by factors of 2 to 5 would have minimal consequences.

Observationally, we find no excess of CRGCs in our radio galaxy fields. These 26 fields represent 16% of our survey solid angle which leads to an expected number of four CRGCs in these pointed observations. We have identified three CRGCs in these fields, with one of our CRGCs being the targeted radio galaxy 3C 280 (CRGC 20). This slight under-enhancement of CRGCs is not statistically significant.

Our surveyed sample of WFPC2 fields includes 18 pointed observations towards distant rich clusters of galaxies, which are regions of high galaxy density. However, the environment associated with rich clusters is not conducive to the production of ring galaxies for two reasons. First, the galaxy populations in the core regions of these clusters is predominantly gas-poor E/S0 galaxies in which the star formation that produces the ring structure cannot occur. Second, while the high galaxy density certainly results in more galaxy encounters, the velocity dispersions of rich clusters are also very high ($\sim$1000 km s^{-1}). The relative velocity of the galaxies in these encounters will be considerably large, on the order of several times this dispersion, while the production of collisional ring galaxies results from relatively low velocity ($\sim$200-300 km s^{-1}) encounters (Lynds & Toomre 1976; Appleton & Struck-Marcell 1996; Struck 1999) The low relative velocity, indicative of bound groups of galaxies rather than rich clusters, allows the intruder galaxy to be present for a relatively long period of time, resulting in a significant gravitational impulse on the stars in the target galaxy. For example, the "grand design" spiral structure of M51 is thought to have been produced by an encounter similar to those that produce collisional ring galaxies except for the fact that the companion to M51 (NGC 5195) has passed near the edge of the disk rather than through the center of the disk (Toomre & Toomre 1972). It is also due to the requirement of low relative velocities in these encounters to produce ring galaxies that it is expected these galaxies will merge on a relatively short time scale, hence the reason for using CRGs in this program. The high velocity encounters in clusters are of too short a duration to produce the necessary gravitational affect on the stars in the target galaxy.

We have identified five CRGCs in the 18 fields pointed towards the clusters of galaxies, an area that is 11% of our total surveyed area. Based on this percentage, the expected number of CRGCs in these fields is only 2.8, suggestive of only a slight enhancement of CRGCs in these cluster fields. Of these five CRGCs, two have measured redshifts, with one being at the redshift of the cluster (CRGC 2 with the 3C 295 cluster) and one being beyond the cluster (CRGC 5) and possibly being slightly gravitationally lensed by the foreground cluster.

The large majority of these distant clusters were observed because they exhibit the "Butcher-Oemler" effect, an excess of blue galaxies compared to local clusters of similar richness (Butcher & Oemler 1978, 1985). Spectroscopic observations of the clusters with the largest blue galaxy fractions ($\sim$20%) has revealed that only one-half of the blue galaxies in the fields of these clusters are actually associated with the clusters (Lavery & Henry 1986; Dressler & Gunn 1992). This is consistent with our meager spectroscopic data (1 of 2 galaxies are associated with the cluster). Applying the spectroscopic statistics to our sample of five CGRCs to remove the cluster CRGCs would decrease our CRGC sample by 2 or 3 galaxies, leading to a decrease in the value of m by $\sim$0.2.

It should be noted that despite their possible association with rich clusters, these CRGCs may still be indicative of the properties of the field rather than the cluster environment. The most likely explanation for the presence of the blue star-forming galaxies in these rich clusters is the recent infall of groups, or clouds, of field galaxies associated with these clusters (Lavery & Henry 1988; Lavery et al. 1992b; Ellingson et al. 2001). This scenario is supported by the large velocity dispersion observed for this blue galaxy population (Henry & Lavery 1987; Dressler & Gunn 1992).

4.5. Cosmology

At the present time, it seems that the standard Friedman models of a decelerating universe do not match the observational evidence, based on Type Ia supernovae, which suggests rather that the Universe is now in a stage of acceleration. Prior to the discovery of the "dark energy" contribution to the expansion of the Universe, the observational constraints on the "standard" cosmological model were consistent with $\Omega_M = 0.27$ and $\Omega_\Lambda = 0$. In this cosmological model, while the estimated redshifts of our CRGC sample are slightly larger (see Figure 3), the total volume in the redshift interval of $0.1 \leq z \leq 1$ is $\sim$45% smaller. Therefore, the expected number of CRGCs increases for the various values of m, as shown in Table 2. Our observational result would have produced a larger value of m, with $m = 6.0$. This value of m is the most appropriate for comparing our results with previous determinations for the

value of m which used the $\Omega_\Lambda = 0$ cosmology.

4.6. Summary

Overall, there are several corrections and biases that affect of determination of m. However, those that would lead to a lower value of m are corrections of ~ 0.2, while those leading to a higher value of m are much larger, being $\sim$1-2. This leads us to conclude that our value of m is more likely a minimum value and could easily be an additive factor of 1 or 2 larger. If we make corrections for all the factors above (reduce the local CRG density by a factor of 3, remove the cluster fields from the solid angle and remove the CRGCs identified in these cluster fields, reduce the new solid angle by 10%, and use the k-correction of an Scd galaxy which produces the lowest incompleteness estimate) and correct for incompleteness as described above, we find the value of m to be 7.9.

5. Conclusions

We have identified a total of 25 collisional ring galaxy candidates in 162 *HST* WFPC2 fields. This surprisingly large number of CRGCs implies a galaxy interaction/merger rate that increases very steeply with redshift. We find a minimum value for m of 5.2 ± 0.7, with m possibly being as high as 7 or 8. This large number of distant CRGCs is inconsistent low values of m ($0 \leq m \leq 2$).

Our large value of m may also be influenced by several other evolutionary effects worthy of future investigation. First, the frequency of various types of interactions may be changing, with there being an increase in low angular momentum, highly radial galaxy collisions as a function of redshift. Such collisions are of the type needed for the production of a collisional ring galaxy. Second, evolution of the "target" galaxy population, such that gas-rich disk systems, required to sustain an expanding ring of star formation, would constitute a significantly higher fraction of the field population at $z \sim 1$ than locally.

REFERENCES

Appleton, P. N., & Struck-Marcell, C. 1996, Fundamentals of Cosmic Physics, 16, 111

Appleton, P. N., & Marston, A. P. 1997, AJ, 113, 201

Arp, H. C., & Madore, B. F. 1987, *Catalogue of Southern Peculiar Galaxies and Associations*, Vol. I and II, Cambridge University Press, Cambridge, UK

Bennett, C. L. et al. 2003, ApJS, 148, 1

Bothun, G. D., Schombert, J. M., Impey, C. D., Sprayberry, D., & McGaugh, S. S. 1993, AJ, 106, 530

Boyle, B. J., Shanks, T., & Peterson, B. A. 1988, MNRAS, 235, 935

Broadhurst, T. J., Ellis, R. S., & Glazebrook, K. 1992, Nature, 355, 55

Burkey, J. M., Keel, W. C., Windhorst, R. A., & Franklin, B. E. 1994, ApJ, 429, L13

Butcher, H., & Oemler, A. Jr. 1978, ApJ, 226, 559

Butcher, H., & Oemler, A. Jr. 1985, ApJ, 290, 496

Carlberg, R. G. 1990, ApJ, 359, L1

Carlberg, R. G. & Charlot, S. 1992, ApJ, 397, 5

Carlberg, R. G., Pritchet, C. J., & Infante, L. 1994, ApJ, 435, 540 (CPI)

Carroll, S. M., Press, W. H., & Turner, E. L. 1992, ARA&A, 30, 499

Cohen, J. G., Cowie, L. L., Hogg, D. W., Songaila, A., Blandford, R., Hu, E. M., & Shopbell, P. 1996, ApJ, 471, L5

Colin, P., Schramm, D. N., & Peimbert, M. 1994, ApJ, 426, 459

Conselice, C., Bershady, M. A., Dickinson, M., & Papovich, C. 2003, AJ, 126, 1183

Couch, W. J., Ellis, R. S., Sharples, R. M., & Smail, I. 1994, ApJ, 430, 121

Dressler, A., & Gunn, J. E. 1983, ApJ, 270, 7

Dressler, A., & Gunn, J. E. 1992, ApJS, 78, 1

Dressler, A., Oemler, A. J., Sparks, W. B., & Lucas, R. A. 1994, ApJ, 435, L23

Ellingson, E., Lin, H.. Yee, H. K. C.. & Carlberg, R. G. 2001, ApJ, 547, 609

Few, J. M., & Madore, B. F. 1986, MNRAS, 222, 673 (FM86)

Freeman, K. C., & de Vaucouleurs, G. 1974, ApJ, 194, 568

Gioia, I. M., Shaya, E. J., Le Fèvre, O., Falco, E. E., Luppino, G. A., & Hammer, F. 1998, ApJ, 497, 573

Harvanek, M., Ellingson, E., Stocke, J. T., & Rhee, G. 2001, ApJ, 122, 2874

Henry, J. P., & Lavery, R. J. 1987, ApJ, 323, 473

Hibbard, J. E., & Vacca, W. D. 1997, AJ, 114, 1741

Hill, G. J., & Lilly, S. J. 1991, ApJ, 367, 1

Holtzman, J. A., et al., 1995, PASP, 107, 156

Lavery, R. J., & Henry, J. P. 1986 ApJ, 304, L5

Lavery, R. J., & Henry, J. P. 1988, ApJ, 330, 596

Lavery, R. J., & Mighell, K. J. 1992, AJ, 103, 81

Lavery, R. J., Pierce M. J., & McClure, R. D. 1992b, AJ, 104, 2067

Lavery, R. J., Seitzer, P., Suntzeff, N. B., Walker, A. R., & Da Costa, G. S. 1996, ApJ, 467, L1

Lavery, R. J. & Remijan, A. J. 2000, ASP Conf. Ser. 197: Dynamics of Galaxies: from the Early Universe to the Present, 327

Le Fèvre, O., Abraham, R., Lilly, S. J., Ellis, R. S., Brinchann, J., Schade, D., Tresse, L., Colless, M., Crampton, D., Glazebrook, K., Hammer, F., & Broadhurst, T. 2000, MNRAS, 311, 565

Lonsdale, C. J., Hacking, P. B., Conrow, T. P., & Rowan-Robinson, M. 1990, ApJ, 358, 60

Luppino, G. A., Gioia, I. M., Annis, J., Le Fèvre, O., & Hammer, F. 1993, ApJ, 416, 444

Lynds, R., & Toomre, A. 1976, ApJ, 209, 382

Mihos, C. 1995, ApJ, 438, 75

Neuschaefer, L. W., Ratnatunga, K. U., Griffiths, R. E., Casertano, S., & Im, M. 1995, ApJ, 453, 559

Oke, J. B. 1990, AJ, 99, 1621

Patton, D. R., Pritchet, C. J., Yee, H. K. C., Ellingson, E., & Carlberg, R. G. 1997, ApJ, 475, 29

Patton, D. R., et al. 2002, ApJ, 565, 208

Pence, W. 1976, ApJ, 203, 39

Schweizer, F. 1983, IAU Symposium, 100, 319

Schweizer, F., & Seitzer, P. 1992, AJ, 104, 1039

Spinrad H., Djorgovski S., Marr J., & Aguilar L. 1985, PASP, 97, 932

Struck, C. 1999, Physics Reports, 321, 1

Thompson, L. 1977, ApJ, 211, 684

Toomre, L., & Toomre, A. 1972, ApJ, 405, 142

Toomre, L. 1977, in "The Evolution of Galaxies and Stellar Population", eds. B.M. Tinsley & R.B. Larson, 401

Woods, D., Fahlman, G. G., & Richer, H. B. 1995, ApJ, 454, 32

Yates, M. G., Miller, L., & Peacock, J. A. 1989, MNRAS, 240, 129

Yee, H. K. C., & Ellingson, E. 1995, ApJ, 445, 37

Zepf, S. E., & Koo, D. C. 1989, ApJ, 337, 34

Zirbel, E. L. 1997, ApJ, 476, 489

Zwicky, F. 1941, in Theodore von Karman Anniversary Volume, Contribution to applied Mechanics and Related Subjects, Caltech, Pasadena, CA, p. 137

Table 1.   Observed Properties of Collisional Ring Galaxies Candidates (CRGCs)

CRGC #	RA (J2000)	DEC (J2000)	m_B (mag)	m_V (mag)	m_R (mag)	m_I (mag)	B-V (mag)	V-R[a] (mag)	V-I[a] (mag)	z_{est}	z_{obs}
1	02:39:58.2	-01:36:59	$\cdots$	22.98	$\cdots$	21.32	$\cdots$	$\cdots$	1.66	0.67	$\cdots$
2	14:11:11.7	+52:12:01	$\cdots$	$\cdots$	20.34	$\cdots$	$\cdots$	1.00	$\cdots$	0.43	0.454
3	12:36:57.2	+62:12:26	$\cdots$	23.02	$\cdots$	$\cdots$	$\cdots$	$\cdots$	$\cdots$	0.68	0.561
4	02:40:55.1	-08:22:17	$\cdots$	$\cdots$	$\cdots$	21.02	$\cdots$	$\cdots$	1.50	0.59	$\cdots$
5	04:43:11.2	+02:10:12	$\cdots$	$\cdots$	21.62	$\cdots$	$\cdots$	1.00	$\cdots$	0.61	0.532
6	21:40:14.0	-23:40:17	$\cdots$	$\cdots$	22.52	$\cdots$	$\cdots$	1.00	$\cdots$	0.79	$\cdots$
7	07:50:46.8	+14:40:46	$\cdots$	22.72	$\cdots$	21.30	$\cdots$	$\cdots$	1.42	0.63	0.629[b]
8	06:11:16.4	-48:48:29	23.67	23.45	$\cdots$	21.74	0.22	$\cdots$	1.71	0.76	$\cdots$
9	03:06:16.3	+17:20:28	$\cdots$	$\cdots$	21.92	$\cdots$	$\cdots$	1.00	$\cdots$	0.66	$\cdots$
10	10:07:58.8	+07:30:09	$\cdots$	$\cdots$	22.54	$\cdots$	$\cdots$	1.00	$\cdots$	0.79	0.580
11	17:09:59.8	+10:32:02	$\cdots$	23.53	$\cdots$	$\cdots$	$\cdots$	$\cdots$	$\cdots$	0.78	$\cdots$
12	16:03:09.1	+42:46:03	$\cdots$	$\cdots$	21.37	$\cdots$	$\cdots$	1.00	$\cdots$	0.57	$\cdots$
13	04:56:47.2	+03:52:32	$\cdots$	$\cdots$	$\cdots$	21.97	$\cdots$	$\cdots$	1.50	0.77	$\cdots$
14	18:07:01.4	+45:44:12	$\cdots$	23.34	$\cdots$	21.73	$\cdots$	$\cdots$	1.61	0.74	$\cdots$
15	10:47:53.3	-25:14:08	$\cdots$	$\cdots$	$\cdots$	22.25	$\cdots$	$\cdots$	1.50	0.83	$\cdots$
16	13:15:22.3	+49:09:25	$\cdots$	$\cdots$	$\cdots$	22.48	$\cdots$	$\cdots$	1.50	0.89	$\cdots$
17	07:27:42.8	+69:06:47	$\cdots$	20.64	$\cdots$	19.37	$\cdots$	$\cdots$	1.27	0.35	$\cdots$
18	02:40:57.4	-08:23:25	$\cdots$	$\cdots$	$\cdots$	19.42	$\cdots$	$\cdots$	1.50	0.38	$\cdots$
19	12:30:19.0	+12:21:54	$\cdots$	22.94	$\cdots$	$\cdots$	$\cdots$	$\cdots$	1.50	0.66	$\cdots$
20	12:56:57.8	+47:20:20	$\cdots$	$\cdots$	22.04	$\cdots$	$\cdots$	1.00	$\cdots$	0.68	0.996
21	02:39:58.4	-01:36:34	$\cdots$	22.65	$\cdots$	21.28	$\cdots$	$\cdots$	1.37	0.61	$\cdots$
22	19:38:09.0	-46:20:48	$\cdots$	23.59	$\cdots$	21.83	$\cdots$	$\cdots$	1.77	0.80	$\cdots$
23	02:40:55.1	-08:22:43	$\cdots$	$\cdots$	$\cdots$	21.78	$\cdots$	$\cdots$	1.50	0.73	$\cdots$
24	15:06:26.7	+01:43:11	$\cdots$	23.81	$\cdots$	21.91	$\cdots$	$\cdots$	1.90	0.85	$\cdots$
25	12:50:02.1	+39:52:21	$\cdots$	$\cdots$	$\cdots$	19.93	$\cdots$	$\cdots$	1.50	0.44	$\cdots$

[a]Since a V-band magnitude is necessary for the redshift estimation, when no V-band image was available, we have assumed a color of V-$R = 1.00$ or V-$I = 1.50$ to determine the m_V from m_R or m_I. The ":" indicates an uncertain redshift.

[b]This redshift is uncertain.

Table 2.   Expected Number of CRGs

Exponent m	Number of CRGs $\Omega_M = 0.27,\ \Omega_\Lambda = 0.73$	Number of CRGs $\Omega_M = 0.27,\ \Omega_\Lambda = 0$
0	1.4	0.8
1	2.4	1.4
2	4.1	2.5
3	7.2	4.3
4	12.8	7.6
5	22.9	13.6
6	41.5	24.6
7	75.6	44.7
8	138.8	81.9

Note. — In the above table we present the number of CRGs expected to be detected in our survey as a function of the merger rate exponent m for two different sets of cosmological parameters of a flat universe ($\Omega_k = 0$). Note that our results are independent of the value of the Hubble constant H_0 (see Section 3.2).
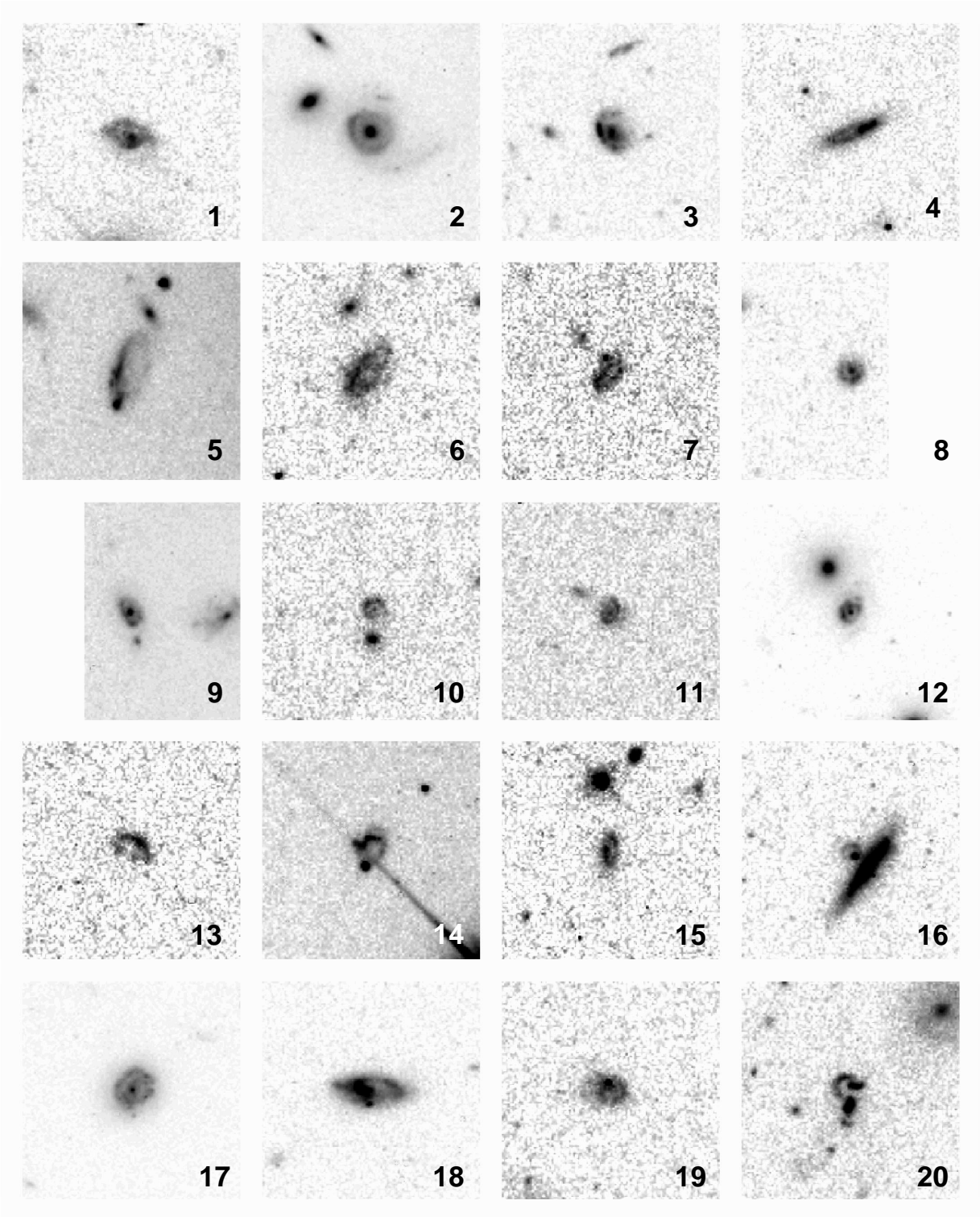
Fig. 1.— *HST* WFPC2 images of 20 of our identified CRGCs. Each galaxy is identified by an index number at the bottom right corner as given in Table 1. These images were extracted from the broad *HST R*-band or *I*-band (F606W, F622W, F702W, F814W) data sets used in the identification process. Each image in the panel is 10 by 10 arcseconds.
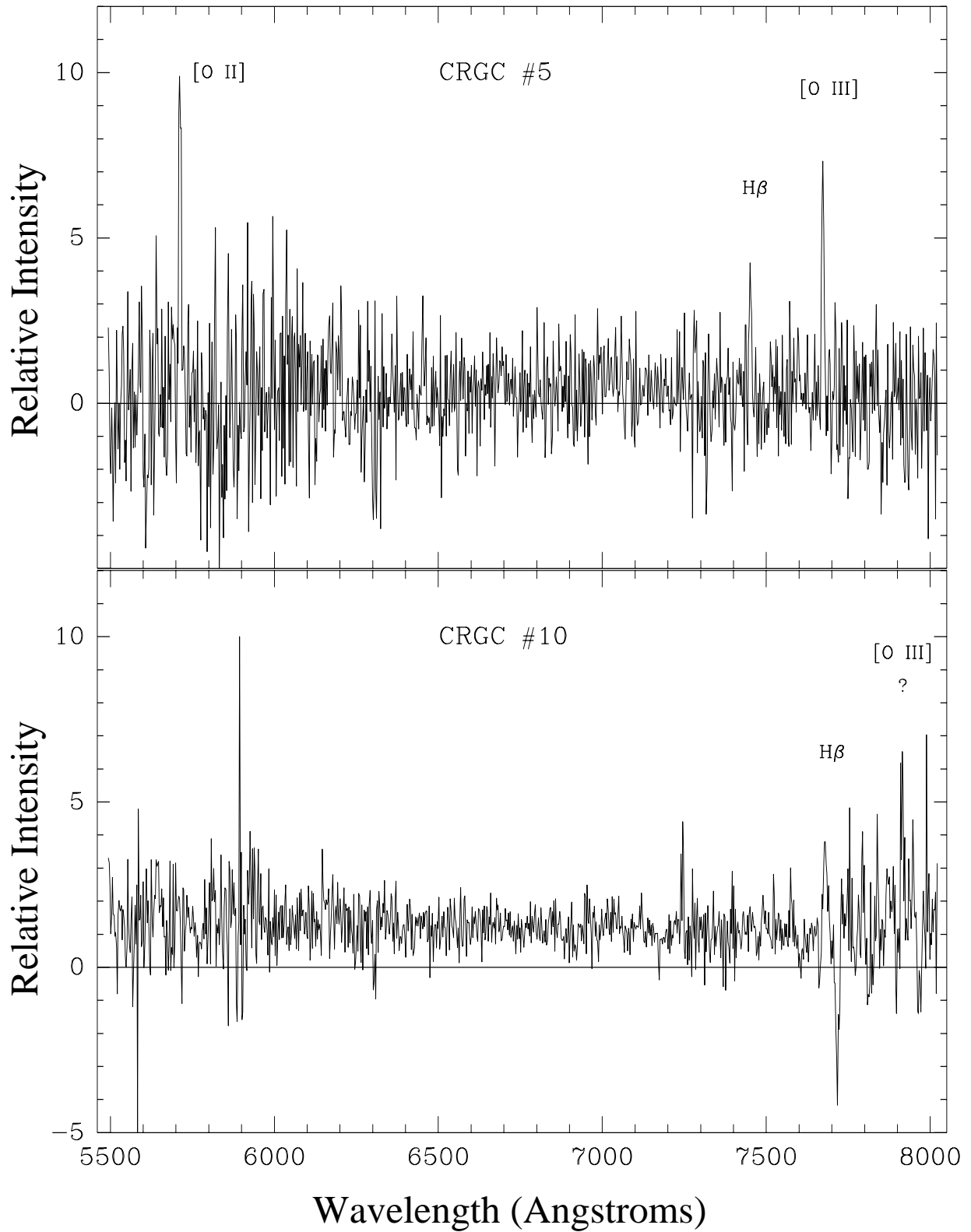
Fig. 2.— Spectra of CRGC #5 ($z = 0.532$) and #10 ($z = 0.580$) obtained with the Palomar 5.0-meter telescope.
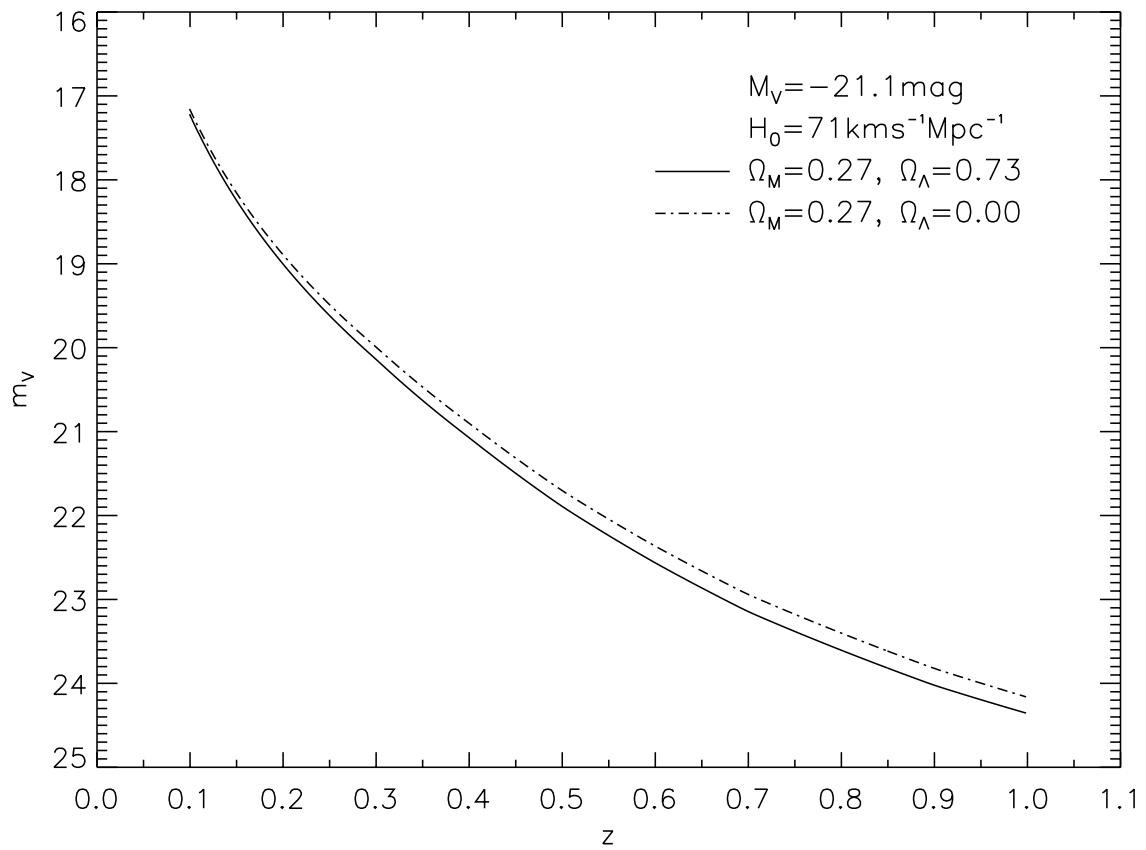
Fig. 3.— Apparent V magnitude versus redshift for a "standard" absolute V magnitude ring galaxy for two cosmological models. The solid curve was used to determine the estimated redshifts given in Table 1.
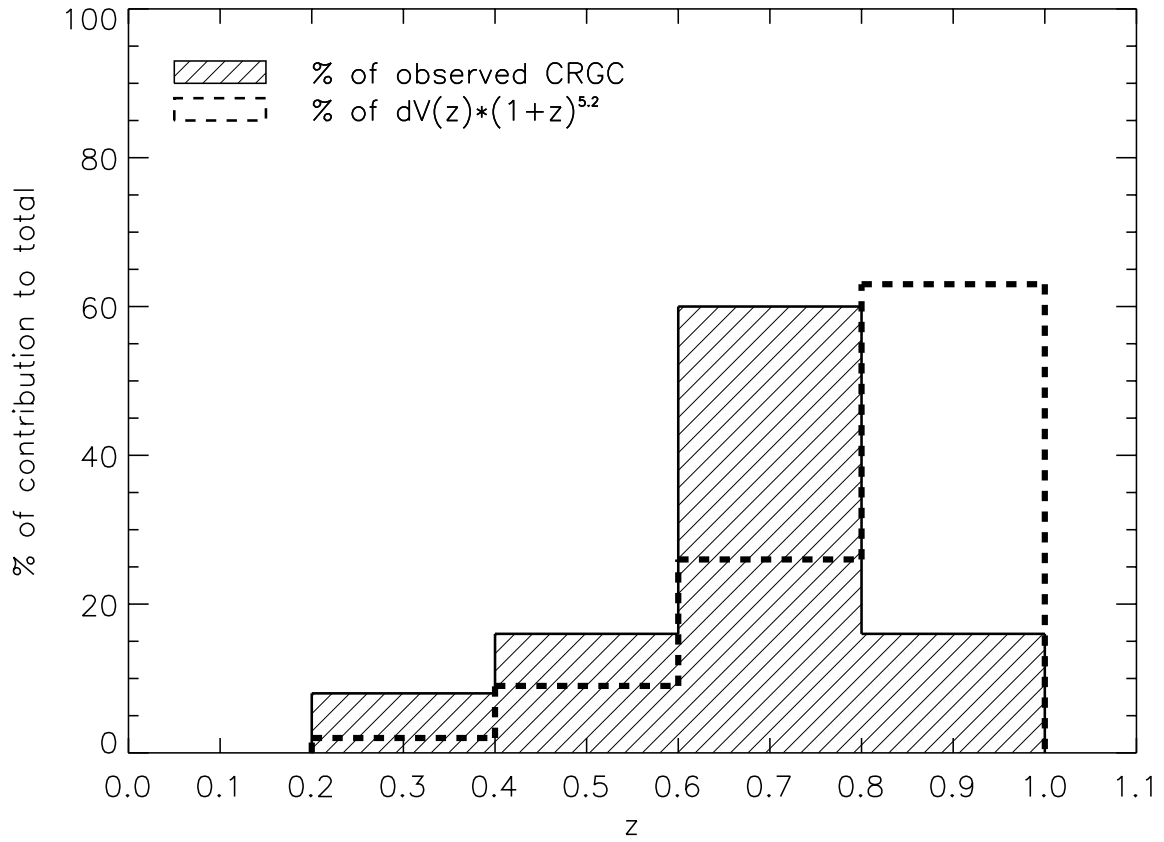
Fig. 4.— Histogram of the percentage distribution of our CRGC sample with redshift (hatched histogram) compared with the percentage distribution of the product of the co-moving volume and evolutionary factor (broken-line histogram).